Nonthermal equilibrium states of closed bipartite systems

Harry Schmidt* and Günter Mahler
Institut für Theoretische Physik 1, Universität Stuttgart, Stuttgart, Germany

(Received 30 January 2007; published 12 June 2007)

We investigate a two-level system in resonant contact with a larger environment. The environment typically is in a canonical state with a given temperature initially. Depending on the precise spectral structure of the environment and the type of coupling between both systems, the smaller part may relax to a canonical state with the same temperature as the environment (i.e., thermal relaxation) or to some other quasiequilibrium state (nonthermal relaxation). The type of (quasi)equilibrium state can be related to the distribution of certain properties of the energy eigenvectors of the total system. We examine these distributions for several abstract and concrete (spin environment) Hamiltonian systems; the significant aspect of these distributions can be related to the relative strength of the local and interaction parts of the Hamiltonian.

DOI: 10.1103/PhysRevE.75.061111 PACS number(s): 05.30.−d, 03.65.Yz, 75.10.Jm

I. INTRODUCTION

In a composite but closed quantum system in which a smaller central system S is weakly coupled to a larger environment C, most of the (pure) states of the total system for a given energy (and possibly some additional constraints) exhibit properties of thermal equilibrium states with respect to the smaller part [1]; i.e., there exists a so-called dominant region in Hilbert space in which the entropy of the central system is close to its maximum value under the given constraints. Therefore, for most pure initial states of the total system, the state of the central system shows decoherence and some kind of thermalization; it typically approaches a quasiequilibrium canonical state with a temperature given by the spectral properties of the environment [2].

If the environment initially is in a thermal state with a given temperature and consists of many bands or of a broad continuum of levels, the central system typically relaxes to a thermal state with the same temperature. This type of relaxation will be called *thermal* relaxation in the following. Here we investigate to what extent certain structures of the total system influence the reached (quasi)equilibrium state. We will relate this equilibrium state to the distribution of the energy eigenvectors of the system, or rather certain important aspects of this distribution. We will show that there is a close relation between the two and how this affects the equilibrium state for different system structures.

We particularly focus on a single spin-1/2 particle coupled to an environment of spin-1/2 particles. Recently, the properties of the spin systems of different structure (rings, stars, and others) have been the subject of extensive interest. A lot of work has been done on the question of entanglement [3–8], their relaxation behavior has been addressed [9,10], and various techniques were suggested to make any spin interact with any other spin [11,12].

Here we extend our analysis from our previous paper [13] regarding the controllability of the relaxation behavior within these spin systems

*Electronic address: harry.schmidt@itp1.uni-stuttgart.de

II. CANONICAL AND NONCANONICAL RELAXATION

Figure 1 shows a two-level system (TLS) in resonant ($\delta_S = \delta_C = \delta$) contact with an environment consisting of two "energy bands" k and k' of degeneracies g_k and $g_{k'}$, respectively (for simplicity we use $g = g_k$, $g' = g_{k'}$ in the following, typically $g' > g$). The coupling is assumed to be weak; the total system is described by the Hamiltonian

$$\hat{H} = \hat{H}_S + \hat{H}_C + \hat{H}_{\text{int}}.$$

A nonequilibrium state $|1\rangle_S \otimes |\phi_k\rangle_C$ is depicted (here $|\phi_k\rangle$ denotes an arbitrary pure environmental state in band k).

If this state is taken as the initial state of a Schrödinger time evolution of the total system, a relaxation to an equilibrium situation is expected in which the time-averaged reduced-state operator of S is given by [1]

$$\hat{\rho}_S = \frac{1}{g + g'} (g' |0\rangle\langle 0| + g |1\rangle\langle 1|), \tag{1}$$

which can be interpreted as a canonical-state operator with inverse temperature:

$$\beta_S = \frac{1}{k_B T} = \frac{1}{\delta_S} \ln \frac{g'}{g}.$$

For a finite environment and weak random coupling, the reduced state of the central system after relaxation still fluctuates around Eq. (1); see [2].

If the central system relaxes to state (1) for any pure state $|\phi_k\rangle$ of the environment in band k, it will relax to the same state for an initial state in which the environment is com-

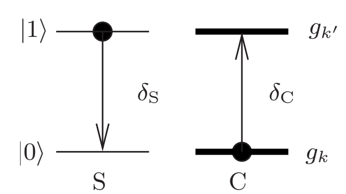

FIG. 1. A two-level system S in contact with an environment C consisting of two highly degenerate levels k and k' with degeneracies g_k and $g_{k'}$.

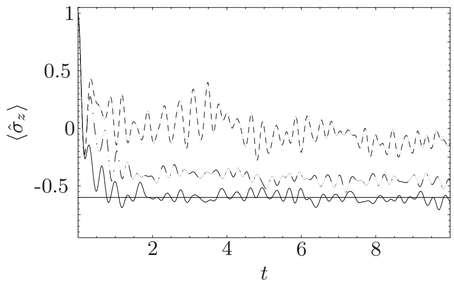

FIG. 2. z component of the Bloch vector of S for the initial state depicted in Fig. 1. The environment consists of spins that are randomly coupled to the central spin. Mutual coupling between the environmental spins is strong (bottom curve), weak (middle curve), or nonexistent (top curve). Fluctuations are due to the finite size of the system. The black line indicates canonical equilibrium. The unit of time is of little importance here as it can be adjusted by adjusting the strength of $\hat{H}_{\text{int}}$. For additional discussion of the model and the time unit see [13].

pletely mixed within band k, $\hat{\rho}_0=|1\rangle\langle 1|\otimes\frac{\hat{1}_k}{g}$. Here $\hat{1}_k$ denotes the projector onto band k of the environment.

Assume now that the environment is given by a large number N of two level systems with a homogeneous Zeeman splitting, $\hat{H}_C=\sum_{i=1}^{N}\delta\hat{\sigma}_z^{(i)}$. The environment initially is taken to be in a thermal state of temperature β_C,

$$\hat{\rho}_0 = |1\rangle\langle 1| \otimes \frac{1}{Z}e^{-\beta_C \hat{H}_C}.$$

If each band of the environment separately leads to a relaxation into a state (1), the equilibrium state of the central system is given by the canonical state with $\beta_S=\beta_C$ for large N. For finite N, the population of the excited state of S after relaxation is given by

$$(\hat{\rho}_S)_{11} = \frac{N}{N+1}\frac{1}{1+e^{\delta\beta_C}} + \frac{1}{N+1} \xrightarrow[N\gg 1]{} \frac{1}{1+e^{\delta\beta_C}}.$$

Because of this, we call the relaxation from an initial state $|1\rangle_S\otimes|\phi_k\rangle_C$ to the reduced equilibrium state (1) *canonical* or *thermal* throughout this text.

However, not all environments lead to canonical relaxation of the central system. In [13] we examined several types of spin environments and showed that many of these lead to an equilibrium state that differs from Eq. (1). We call these deviations noncanonical or nonthermal. Figure 2 shows the relaxation behavior for different types of environments. Obviously, not all relax to the same quasiequilibrium state.

III. ENERGY EIGENVECTOR DISTRIBUTIONS

We now correlate deviations from canonical relaxation with the distribution of the energy eigenvectors of the total system. We only consider the situation depicted in Fig. 1, since environments with more bands in a canonical state can simply be derived from these results. As long as the interaction is weak relative to the band splitting, the total system can be reduced to the subspace consisting of the "cross states:"

$$\{|0_S, \text{environment in band } k'\rangle,$$

$$|1_S, \text{environment in band } k\rangle\}. \tag{2}$$

In the following we will always refer only to this $(g+g')$-dimensional subspace.

Instead of the temperature, we consider the population inversion $\text{Tr}\{\hat{\sigma}_z\hat{\rho}_S\}$ of the central system for mathematical convenience. The inversion of the canonical state (1) is given by

$$\langle\hat{\sigma}_z\rangle_{\text{can}} = \frac{g-g'}{g+g'}.$$

The energy eigenvectors can be written in the form

$$|\varepsilon\rangle \approx \alpha_\varepsilon|0,\chi_\varepsilon\rangle + \beta_\varepsilon|1,\eta_\varepsilon\rangle, \tag{3}$$

where $|\chi_\varepsilon\rangle$ is a state in band k' and $|\eta_\varepsilon\rangle$ a state in band k of the environment. In the following we will use ε as a discrete index running from 1 to $g+g'$ to number the energy eigenvectors within the subspace of Hilbert space spanned by the states (2).

We expand the initial state $\hat{\rho}_0=|1\rangle\langle 1|\otimes\frac{\hat{1}_k}{g}$ in terms of these eigenvectors, $\hat{\rho}_0=\sum_{\varepsilon,\varepsilon'}\rho_{0,\varepsilon\varepsilon'}|\varepsilon\rangle\langle\varepsilon'|$. Averaging over all times and tracing out the environment yields the equilibrium state of the central system,

$$\bar{\rho}_S = \sum_\varepsilon \rho_{0,\varepsilon\varepsilon}\text{Tr}_C\{|\varepsilon\rangle\langle\varepsilon|\} = \sum_\varepsilon |\beta_\varepsilon|^2(|\alpha_\varepsilon|^2|0\rangle\langle 0| + |\beta_\varepsilon|^2|1\rangle\langle 1|).$$

The respective inversion is

$$\langle\bar{\sigma}_z\rangle = \sum_\varepsilon |\beta_\varepsilon|^2(|\beta_\varepsilon|^2 - |\alpha_\varepsilon|^2).$$

We notice that

$$\lambda_\varepsilon = |\beta_\varepsilon|^2 - |\alpha_\varepsilon|^2 \tag{4}$$

is the inversion of $|\varepsilon\rangle$. Since $|\beta_\varepsilon|^2+|\alpha_\varepsilon|^2=1$, we can rewrite the time-averaged inversion of the central system completely in terms of the λ_ε's,

$$\langle\bar{\sigma}_z\rangle = \frac{1}{2}\left(\sum_\varepsilon \lambda_\varepsilon + \sum_\varepsilon \lambda_\varepsilon^2\right).$$

The first sum can be shown to be equal to $g-g'$; see Appendix A. If we rewrite the second sum in terms of the variance $\Delta\lambda_\varepsilon^2$ of the λ_ε distribution, we finally get

$$\langle\bar{\sigma}_z\rangle = \langle\hat{\sigma}_z\rangle_{\text{can}} + \frac{(g+g')}{2g}\Delta\lambda_\varepsilon^2. \tag{5}$$

The average deviation from the canonical equilibrium state is thus mainly given by the distribution of the reduced states of the energy eigenvectors, in particular by its variance.

As long as the width of the distribution is finite, there is always a deviation from the canonical inversion and therefore also from the canonical temperature. For a finite environment this is always the case. We will now consider several types of environments and interactions.

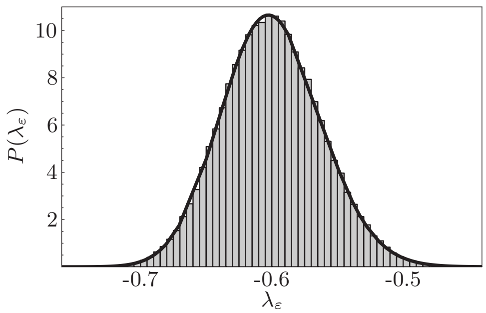

FIG. 3. λ_ε distribution for random Hermitian matrices from the GUE. The solid line shows the (normalized) probability density (6); the histogram is calculated form the eigenvectors of 400 different random matrices. $g=91$, $g'=364$, $\Delta\lambda_\varepsilon^2=2/1425\approx 0.0014$, and $\langle\hat{\sigma}_z\rangle_{\text{can}}=-0.6$.

IV. EIGENVECTOR DISTRIBUTION FOR DIFFERENT HAMILTONIANS

A. Random Hamiltonian

At first we assume that the two relevant bands in the environment are exactly degenerate and the transitions within S and C are exactly in resonance. In this case, $\hat{H}_S+\hat{H}_C\propto\hat{1}$ [within the relevant subspace spanned by the states (2)]; thus, we only need to deal with $\hat{H}_{\text{int}}$.

If the coupling $\hat{H}_{\text{int}}$ between system and environment is modeled by a random Hermitian matrix with a uniform Gaussian distribution $w(\hat{H}_{\text{int}})=C\exp(-A\text{Tr}\{\hat{H}_{\text{int}}\}^2)$ [i.e., taken from the Gaussian unitary ensemble (GUE) [14]], the state of the central system typically relaxes to the expected equilibrium state under Schrödinger dynamics for the total system [1,2,13]. The state fluctuates in time; the amplitude of these fluctuations decreases with the size of the environment.

Figure 3 shows the λ_ε distribution for these random Hermitian matrices. The histogram was obtained by choosing a number of random matrices with the given probability distribution and calculating the inversion of their eigenvectors. The parameters used are $g=91$ and $g'=364$.

The probability density for the λ_ε's for random Hermitian matrices from the GUE can be calculated analytically and is given by

$$P(\lambda)\propto(1-\lambda)^{g'-1}(1+\lambda)^{g-1}. \tag{6}$$

This result is derived in Appendix B. The solid line in Fig. 3 shows the distribution.

The mean value of λ_ε for this distribution is given by

$$\bar{\lambda}_\varepsilon=\frac{g-g'}{g+g'}=\langle\hat{\sigma}_z\rangle_{\text{can}},$$

as expected from the general result in Appendix A. This is again the mean inversion of the equilibrium state for canonical relaxation.

The variance of this distribution is given by

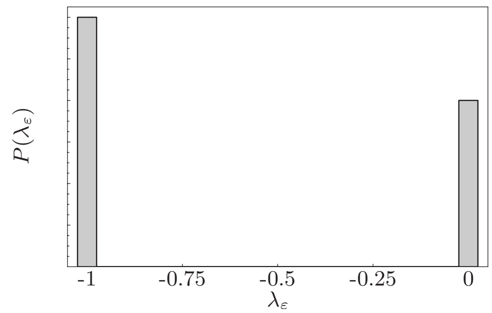

FIG. 4. Random interaction and degenerate bands. The two bars represent δ peaks of different strength. For an explanation of the height of the bars see the text. $\Delta\lambda_\varepsilon^2=6/25=0.24$.

$$\Delta\lambda_\varepsilon^2=4\frac{gg'}{d^2(d+1)},$$

with $d=g+g'$. Since this is finite, the steady state reached will typically deviate from the canonical equilibrium state.

For large systems—i.e., $d\to\infty$ (for constant ratio g/g')—both $\Delta\lambda_\varepsilon^2$ and $\langle\bar{\sigma}_z\rangle-\langle\hat{\sigma}_z\rangle_{\text{can}}$ vanish. So in the thermodynamic limit, the quasiequilibrium reached equals the canonical equilibrium.

B. Random interaction

1. Degenerate bands

We will now discuss a system that is not completely random, but has a random energy exchanging coupling between the central system and the environment. If the environmental bands are strictly degenerate, the Hamiltonian matrix has the form

$$\left(\begin{array}{ccc|ccc} -\Delta/2 & & & & & \\ & \ddots & & & \mathsf{V}^\dagger & \\ & & -\Delta/2 & & & \\ \hline & & & \Delta/2 & & \\ & \mathsf{V} & & & \ddots & \\ & & & & & \Delta/2 \end{array}\right), \tag{7}$$

where $\Delta=\delta^S-\delta^C$ is the detuning between the system and environment. The upper left block corresponds to the ground state of the central system, and it is therefore of dimension g'; the lower right block (of dimension g) corresponds to the excited level. These blocks are purely diagonal.

The off-diagonal block V (a $g\times g'$ matrix), corresponding to energy exchange (canonical) coupling, is chosen randomly with normalized Gaussian distributions for the real and imaginary parts of the matrix elements.

For $\Delta\neq 0$, the system and environment are off resonance and the relaxation to the canonical equilibrium state is prohibited by energy conservation. So just $\Delta=0$ is considered.

Figure 4 shows the λ_ε distribution for a matrix of type (7), again for $g=91$ and $g'=364$. Instead of being single peaked, the distribution here is drastically different and consists of δ peaks at $\lambda_\varepsilon=-1$ and $\lambda_\varepsilon=0$, respectively. For a given Hamiltonian, there are exactly $g'-g$ eigenstates with $\lambda_\varepsilon=-1$ and

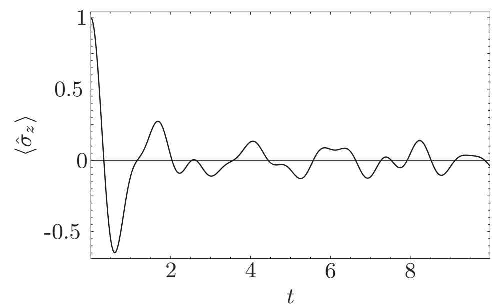

FIG. 5. Time evolution of the z component of the Bloch vector of S for a random interaction and degenerate environmental bands, as described in Sec. IV B 1. Note that the canonical equilibrium state for the given parameters would be at $\langle\hat{\sigma}_z\rangle = -0.6$.

$2g$ eigenstates with $\lambda_\varepsilon = 0$ (assuming $g' > g$). The mean value still is $\bar{\lambda}_\varepsilon = (g-g')/(g+g')$, as expected.

However, the variance of the distribution is obviously considerably larger. For the given parameters $\Delta\lambda_\varepsilon = 0.24$ as opposed to $\Delta\lambda_\varepsilon \approx 0.0014$ for the completely random Hamiltonian. The deviation of the quasiequilibrium state for a Hamiltonian of type (7) from the canonical one is exactly

$$\langle\bar{\sigma}_z\rangle - \langle\hat{\sigma}_z\rangle_{\text{can}} = -\langle\hat{\sigma}_z\rangle_{\text{can}},$$

which is nicely demonstrated in Fig. 5. Since this result is independent of the system size, going to large environments will not change the relaxation behavior other than reducing the amplitude of the fluctuations. Even in the thermodynamic limit the canonical equilibrium state is never reached.

2. Nondegenerate bands

The situation, again, changes if we introduce a finite spacing between the levels within each environmental band. For simplicity we will only consider equidistant levels and equal bandwidths $\delta\varepsilon$ for both bands here. The lowest (and highest) levels of each band in the environment are in resonance with the central system. This system is depicted in Fig. 6 ($\delta_S = \delta_C$ is considered in the following). The Hamiltonian matrix in subspace (2) is given by

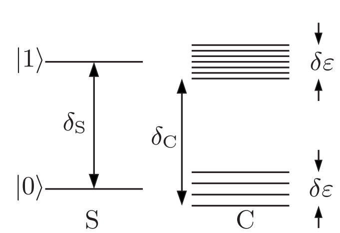

FIG. 6. A TLS in contact with an environment consisting of two "bands" with equidistant level spacing. Both bands have the same width $\delta\varepsilon$; the lower band consists of g levels, the upper band of g' levels.

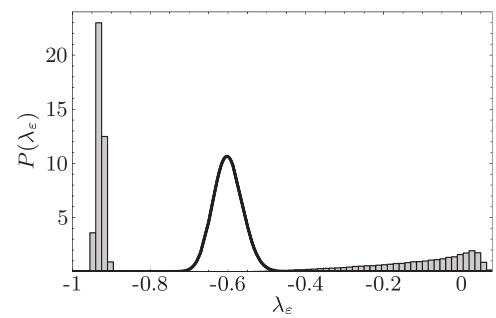

FIG. 7. Random interaction, equidistant spacing, and small level spacing. $\Delta\lambda_\varepsilon^2 \approx 0.19$. The solid line shows the distribution for the complete random Hamiltonian.

$$\left(\begin{array}{cccc|cccc} 0 & & & & & & & \\ & \frac{\delta\varepsilon}{(g'-1)} & & & & \mathsf{V}^\dagger & & \\ & & \ddots & & & & & \\ & & & \delta\varepsilon & & & & \\ \hline & & & & 0 & & & \\ & \mathsf{V}^\dagger & & & & \frac{\delta\varepsilon}{(g-1)} & & \\ & & & & & & \ddots & \\ & & & & & & & \delta\varepsilon \end{array}\right).$$

By introducing a small level splitting in the environment (small compared to the interaction strength), the peaks in Fig. 4 become broader; especially the one at $\lambda_\varepsilon = 0$ becomes flatter considerably and is stretched towards negative λ_ε. The variance of the distribution becomes smaller. Figure 7 shows the λ_ε distribution for a relatively small level spacing.

When the level splitting is increased, the distribution becomes single peaked, with the peak close to its average and of similar height as the peak of the complete random Hamiltonian; see Fig. 8. A long tail towards higher λ_ε prevails; therefore, the variance is still considerably larger.

C. Spin environments

We now consider a gapped spin or TLS as in Fig. 1 coupled to an array of spins, all with a Zeeman splitting

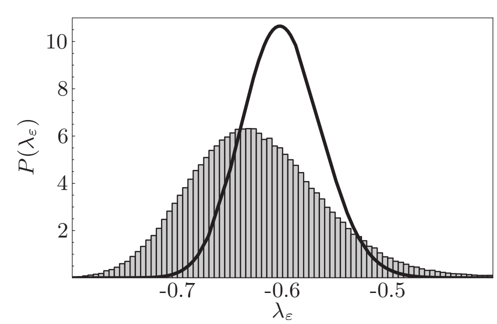

FIG. 8. Random interaction, equidistant spacing, and larger level spacing. The solid line shows the distribution for the complete random Hamiltonian. $\Delta\lambda_\varepsilon \approx 0.022$.

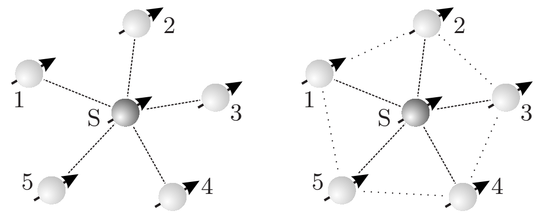

FIG. 9. Schematics of the spin-star (left) and spin-ring (right) configurations. Typically, the environment consists of a lot more than five spins.

equal to the central spin (or almost equal). Due to energy conservation, the system can be reduced to the situation shown in Fig. 1 for each pair of environmental bands. If the environment initially is in a canonical state, we can simply sum up over all bands, as long as the interaction between the environmental spins is small.

The λ_ε distributions of several spin environments have been discussed in [13], so we will only discuss them briefly here.

1. Spin-star configuration

Figure 9 (left) shows schematically a spin-star configuration—i.e., a central spin coupled to an array of environmental spins without mutual interaction. A typical environment should of course consist of a lot more than five spins. The most general Hamiltonian describing the system-environment interaction is

$$\hat{H}_{\text{int}} = \sum_{i,j=1}^{3} \sum_{\nu=1}^{N} \gamma_{ij}^{(\nu)} \hat{\sigma}_i^{(S)} \otimes \hat{\sigma}_j^{(\nu)}$$

for N environmental spins.

It has been shown in [13] that if the coefficients $\gamma_{ij}^{(\nu)}$ are chosen randomly, the initial state depicted in Fig. 4 typically does not relax to the canonical equilibrium state. The Hamiltonian matrix in this case has the form (7); however, with small fluctuations on the diagonal and the interaction part of the Hamiltonian matrix is only sparsely populated. Nevertheless, the λ_ε distribution shows some similarity to the one described in Sec. IV B 2 for small level splitting. Figure 10 shows the λ_ε distribution for this system.

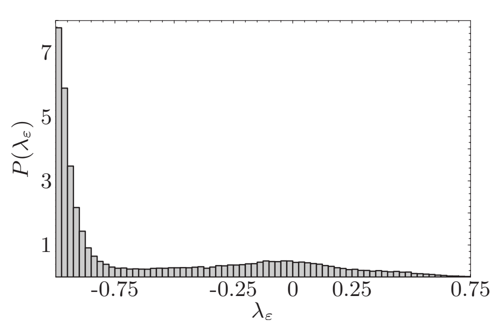

FIG. 10. λ_ε distribution for the spin-star configuration. Fourteen environmental spins and the second and third excited bands are considered, corresponding to $g=91$ and $g'=364$. $\Delta\lambda_\varepsilon^2 \approx 0.216$.

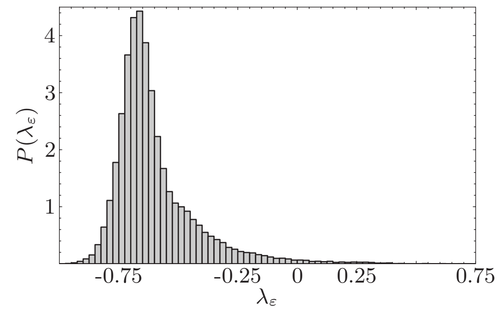

FIG. 11. λ_ε distribution for a spin-ring configuration. Fourteen environmental spins and the second and third excited bands are considered, corresponding to $g=91$ and $g'=364$. $\Delta\lambda_\varepsilon^2 \approx 0.0295$.

2. Intraenvironmental coupling

If the mutual coupling between the environmental spins is introduced, the situation changes. Figure 9 (right) schematically shows next-neighbor coupling in the environment (spin-ring configuration), but other configurations are possible as well. As long as this coupling is weak, the system can still be considered bandwise.

The interaction typically leads to a level splitting within the bands which in turn leads to a λ_ε distribution similar to the one described in Sec. IV B 2 with larger level splitting. Figure 11 shows the λ_ε distribution for a spin-ring configuration. The distribution shown is for a $\hat{\sigma}_x \otimes \hat{\sigma}_x$ next-neighbor coupling. The distributions for different kinds of coupling—e.g., Heisenberg coupling—are similar.

3. Inhomogeneous Zeeman splitting

If the individual environmental spins each have a different Zeeman splitting, the situation becomes similar to the one discussed in Sec. IV B 2. Figure 12 shows the λ_ε distribution when the Zeeman splittings of the environmental spins are homogeneously distributed within a certain range. The distribution again shows a peak around the mean value $\bar{\lambda}_\varepsilon = \langle \hat{\sigma}_z \rangle_{\text{can}}$, although broader than in the previous case.

V. WIDTH OF THE DISTRIBUTION AND SPECTRAL WIDTH

Figures 4, 7, and 8 indicate that there is a continuous transition from a situation far from canonical to an almost

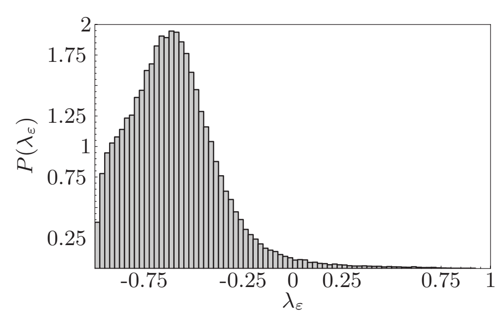

FIG. 12. λ_ε distribution for a spin-star configuration with inhomogeneous Zeeman splitting of the environmental spins. Fourteen environmental spins and the second and third excited bands are considered, corresponding to $g=91$ and $g'=364$. $\Delta\lambda_\varepsilon^2 \approx 0.0548$.

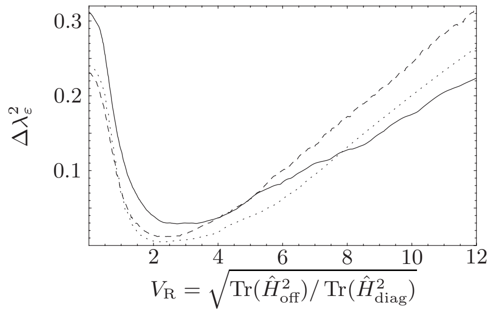

FIG. 13. Variance of the λ_ε distribution over the relative strength of the environmental spectrum for different types of this spectrum. Solid line: spin-ring with random *S-C* coupling. Dashed line: spin-star with random *S-C* coupling and inhomogeneous Zeeman splitting within the environment. Dotted line: spin-star with *XY* coupling between *S* and *C* and inhomogeneous Zeeman splitting within the environment.

canonical relaxation, depending on the environmental spectrum. What has been changed is the "strength" of the environmental spectrum from zero to the minimal variance of the λ_ε distribution. A similar transition can be observed for many different environmental spectra.

In order to relate different types of spectra we split the Hamiltonian matrix (in the considered subspace) in its respective diagonal and off diagonal parts. The off-diagonal part $\hat{H}_{\rm off}$ [V and $\mathsf{V}^\dagger$ of (7)] describes the interaction between central system and environment, while the diagonal part $\hat{H}_{\rm diag}$ describes the environmental spectra alone, if system and environment are in resonance. The diagonal part is always taken to be traceless. The quantity we use to compare different spectra is the relative strength of the environmental part to the interaction part,

$$V_R = \sqrt{\frac{{\rm Tr}(\hat{H}_{\rm diag}^2)}{{\rm Tr}(\hat{H}_{\rm off}^2)}}.$$

For a completely random matrix (GUE) this relation is given on average by

$$V_{R,{\rm GUE}} = \sqrt{\frac{g^2+g'^2}{2gg'}},$$

which only depends on g/g', not on the actual size of the system.

Figure 13 shows the variance of the λ_ε distribution for three different types of environmental spectra. In all three cases the environment consists of 14 spins and the second and third excited bands are considered, $g=91$ and $g'=364$, as described in Sec. IV C.

The solid line corresponds to the spin-ring configuration as described in Sec. IV C 2. The intraenvironmental interaction is taken as a $\hat{\sigma}_x\otimes\hat{\sigma}_x+\hat{\sigma}_y\otimes\hat{\sigma}_y$ next-neighbor coupling; the central system is randomly coupled to each environmental spin. The dashed line corresponds to the configuration described in Sec. IV C 3; there is no mutual interaction between the spins in the environment, but their Zeeman splitting is inhomogeneous. The central system is again coupled randomly to each environmental spin. The environmental spectrum for the dotted line is the same as for the dashed line. However, the interaction between the central spin and each environmental spin is modeled by $\hat{\sigma}_x\otimes\hat{\sigma}_x+\hat{\sigma}_y\otimes\hat{\sigma}_y$. The corresponding average values for a random matrix from the GUE are $\Delta\lambda_\varepsilon^2=2/1425\approx0.0014$ and $V_{R,{\rm GUE}}\approx1.46$, respectively.

We notice that for each type of coupling and environmental spectrum there is a distinct minimum of $\Delta\lambda_\varepsilon^2$ for similar values of V_R close to, but not exactly at, the average value for the GUE matrices.

VI. CONCLUSION

We have characterized situations under which nonthermal states should result as quasiequilibrium states. For a spin-1/2 particle weakly coupled to a larger environment, there is a close relation between the quasiequilibrium state of the small quantum system coupled to a larger environment and the distribution of certain properties of the energy eigenvectors of the total system. The equilibrium state is directly given by the width of this distribution. The spectral structure of the environment and the exact form of the coupling have a strong influence on the eigenvector distribution. To show this we have considered both abstract system Hamiltonians and Hamiltonians for structured spin environments.

Furthermore, there is a close relation between the width of the λ_ε distribution and the strengths of both the local (diagonal) and the interaction (off diagonal) part of the Hamiltonian. By changing certain parameters within each system, there is a distinct minimum of the λ_ε width for a value of the relative strength that is close to the respective value for GUE matrices. This relative strength can thus give an indication whether for a given system relaxation to or close to a thermal state can be expected without calculating the full λ_ε distribution. The relative width gives an indication how to choose the system parameters properly to achieve a certain type of equilibrium situation. This should be of help when designing a spin system for special ("nonthermal") relaxation behavior.

APPENDIX A: TOWARDS Eq. (5)

Here we show that $\sum_\varepsilon\lambda_\varepsilon=g-g'$:

$$\sum_\varepsilon \lambda_\varepsilon = \sum_\varepsilon {\rm Tr}_S\{\hat{\sigma}_z^S {\rm Tr}_C|\varepsilon\rangle\langle\varepsilon|\} = \sum_\varepsilon {\rm Tr}\{(\hat{\sigma}_z^S\otimes\hat{1}^C)|\varepsilon\rangle\langle\varepsilon|\}$$
$$= {\rm Tr}\{(\hat{\sigma}_z^S\otimes\hat{1}^C)\},$$

the last equality following from the fact that the energy eigenvectors are a complete orthonormal basis in Hilbert space. If we now use the basis $\{|0,m'\rangle,|1,m\rangle\}$ to calculate the trace (m and m' denote the levels in band k and k', respectively), we see that the g kets $|1,m\rangle$ yield 1's, while the g' kets $|0,m'\rangle$ yield -1's and the total trace equals $g-g'$.

APPENDIX B: DERIVATION OF Eq. (6)

If we introduce the basis $\{|k:m\rangle\}$ $(1<m\leqslant g_k)$ for the band k and the basis $\{|k':m\rangle\}$ for the band k', we can write the state of the total system as $(g=g_k,\ g'=g_{k'})$

$$|\psi\rangle = \sum_{m=1}^{g'} \psi_{0m}|0\rangle \otimes |k':m\rangle + \sum_{m=1}^{g} \psi_{1m}|1\rangle \otimes |k:m\rangle.$$

The reduced state of the central system becomes

$$\hat{\rho}_S = \mathrm{Tr}_C\hat{\rho} = \sum_{m=1}^{g'} |\psi_{0m}|^2|0\rangle\langle 0| + \sum_{m=1}^{g} |\psi_{1m}|^2|1\rangle\langle 1|.$$

We are interested in the distribution of the inversion of the energy eigenstates of certain Hamiltonians. Since the inversion is determined by the population of each level, we will derive the distribution for the population of the ground state, $p_0=\Sigma_m|\psi_{0m}|^2$.

For simplicity we introduce a single index n to label the amplitudes instead of the double index $0m$ or $1m$. n runs from 1 to $d=g+g'$ (the reduced Hilbert-space dimension). In this notation, $p_0=\Sigma_{n=1}^{g'}|\psi_n|^2$.

We now split the amplitudes into real and imaginary parts, $\psi_n=x_k+\mathrm{i}x_{k+1}$, where $1\leqslant k\leqslant 2g'$ corresponds to $|0\rangle\langle 0|$ and $2g'+1\leqslant k\leqslant 2d$ corresponds to $|1\rangle\langle 1|$; therefore, $p_0=\Sigma_{k=1}^{2g'}x_k$. The combined probability density of the first $2g'$ amplitudes x_k for eigenvectors of random matrices from the GUE is given by [14]

$$P_{\mathrm{a}}(x_1,\ldots,x_{2g'}) = \pi^{-1/2}\frac{\Gamma(d)}{\Gamma(d-g')}\left(1-\sum_{k=1}^{2g'}x_k^2\right)^{d-g'-1}.$$

The desired probability density for the population of the ground state p_0 is given by

$$P_{\mathrm{p}}(p_0) = \int \mathrm{d}^{2g'}x P_{\mathrm{a}}(x_1,\ldots,x_{2g'})\,\delta\left(p_0-\sum_{k=1}^{2g'}x_k^2\right),$$

integrating over the unit sphere in $2g'$-dimensional space. The integral yields

$$P_{\mathrm{p}}(p_0) = \frac{\Gamma(d)}{\Gamma(d-g')\Gamma(g')}p_0^{g'-1}(1-p_0)^{d-g'-1}.$$

Transforming to $\lambda=1-2p_0$ finally gives the probability density (6),

$$P(\lambda) = \frac{1}{2^{d-1}}\frac{\Gamma(d)}{\Gamma(d-g')\Gamma(g')}(1-\lambda)^{g'-1}(1+\lambda)^{d-g'-1}. \tag{6'}$$

[1] J. Gemmer, M. Michel, and G. Mahler, *Quantum Thermodynamics: The Emergence of Thermodynamical Behaviour within Composite Quantum Systems* (Springer, Berlin, 2004).
[2] P. Borowski, J. Gemmer, and G. Mahler, Eur. Phys. J. B **35**, 255 (2003).
[3] H. J. Briegel and R. Raussendorf, Phys. Rev. Lett. **86**, 910 (2001).
[4] K. M. O'Connor and W. K. Wootters, Phys. Rev. A **63**, 052302 (2001).
[5] X. Wang, Phys. Rev. A **66**, 034302 (2002).
[6] A. Hutton and S. Bose, Phys. Rev. A **69**, 042312 (2004).
[7] A. Hutton and S. Bose, e-print arXiv:quant-ph/0408077.
[8] G. Vidal, J. I. Latorre, E. Rico, and A. Kitaev, Phys. Rev. Lett. **90**, 227902 (2003).
[9] H.-P. Breuer, D. Burgarth, and F. Petruccione, Phys. Rev. B **70**, 045323 (2004).
[10] J. Lages, V. V. Dobrovitski, and B. N. Harmon, e-print arXiv:quant-ph/0406001.
[11] A. Imamoḡlu, D. D. Awschalom, G. Burkard, D. P. DiVincenzo, D. Loss, M. Sherwin, and A. Small, Phys. Rev. Lett. **83**, 4204 (1999).
[12] Y. Makhlin, G. Schön, and A. Shnirman, Nature (London) **398**, 305 (1999).
[13] H. Schmidt and G. Mahler, Phys. Rev. E **72**, 016117 (2005).
[14] F. Haake, *Quantum Signatures of Chaos* (Springer, Berlin, 2001).